guidestar had to rely entirely on infrared imaging with TIMMI. Luckily, the nearby bright variable R Leo could be acquired and, after correcting the telescope co-ordinates on this source, the "parking star" could also be acquired. The detector setting was then changed for the reappearance for which the lunar background should be negligible. The final keystroke to start the burstmode for the reappearance was entered on $14^h\ 10^m\ 09^s$ UT. The data acquisition was active for 25 seconds and soon after, the individual images of the sequence were displayed. Excitation was rising when after 300 frames the screen still showed pure background. But then the intensity scaling of the display changed, indicating an increasing signal that soon overwhelmed the background level. With great joy we realised that the reappearance was caught late but not too late. Figure 2 shows the corresponding stack of frames. A more realistic impression can be obtained by watching the MPEG movies available at these URLs:

http://www.ls.eso.org/lasilla/Telescopes/360cat/timmi
http://www.tls-tautenburg.de/research/cw_leo.html and
http://www.arcetri.astro.it/~luna/irc10216.html

The first result presented here is based on the preliminary light curve of the reappearance shown in Figure 3. The one-dimensional brightness profile of CW Leo was derived by deconvolving this light curve with a point-source model according to the Fresnel prescription of diffraction at the lunar limb, taking into account all observational circumstances (spectral and temporal bandwidth, etc.). The deconvolution procedure utilises a maximum-entropy algorithm, which is the same as in Stecklum et al. (1995). The resulting brightness distribution has a FWHM of 0.6″, which confirms previous estimates. The eastern part is more wiggly, presumably due to scintillation, which influenced the last part of the light curve. Figure 4 provides a superposition of the eastern and western parts of the brightness profile. It can be recognised that there are step-like features in the profile, which occur almost symmetrically on either side. At least four such steps can be distinguished. Although the reduction of the data just started, we are confident that these features are not spurious but represent imprints of the innermost dust shells. Furthermore, the profile looks rather flat-topped and is much broader at its peak than the often-adopted angular diameter of the star of 40 mas. This indicates that either the photosphere is much more extended than previously believed or even hidden from direct view at mid-infrared wavelengths.

More in-depth conclusions will be drawn by comparing the final brightness profiles to model calculations. For us observers, the measurement was a breathtaking experience, and for TIMMI, it was a great finale. We'll miss you.

References

Acker, A., Ochsenbein, R., Stenholm, B., Tylenda, R., Marcout, J., & Schon, C., 1992, *Strasbourg-ESO Catalogue of Galactic Planetary Nebulae*, ESO.
Crabtree, D.R., McLaren, R.A., & Christian, C.A., 1987, in: *Late Stages of Stellar Evolution*, eds. S. Kwok & S.R. Pottasch, Kluwer Academic Publ., 145.
Groenewegen, M.A.T., van der Veen, W.E.C.J., Lefloch, B., & Omont, A., 1998, *A&A*, **322**, L21.
Haniff, Ch. & Buscher, 1998, *A&A*, **334**, L5.
Iben, I., & Renzini, A., 1983, *ARA&A*, **21**, 271.
Käufl, H.-U., Jouan, R., Lagage, P.O., Masse, P., Mestreau, P., Tarrius, A., 1992, *The Messenger* **70**, 67.
Käufl, H.-U., Stecklum, B., & Richichi, A., 1998, Proc. SPIE, 3350, p. 267.
Shawl, S.J. & Zellner, B., 1970, ApJ, 162, L19.
Skinner, C.J., Meixner, M., & Bobrowski, M., 1998, *MNRAS*, **300**, L29
Sloan, G.C. & Egan, M.P., 1995, ApJ, 444, 452
Stecklum, B., Henning, T., Eckart, A., Howell, R.R., & Hoare, M., 1995, *ApJ*, **445**, L153.
Stecklum, B., Käufl, H.-U., Richichi, A., 1997, in: Science with the VLTI, ed. F. Paresce, Springer-Verlag, 153.
Toombs, R.L., Becklin, E.E., Frogel, J.A., Law, S.K., Porter, F.C., & Westphal, J.A., 1972, *ApJ*, **173**, L71.
Weigelt, G., Balega, Y., Blöcker, T., Fleischer, A.J., Osterbart, R., & Winters, J.M., 1998, *A&A*, **333**, L51.
Winters, J.M., Fleischer, A.J., Gauger, A., & Sedlmayr, E., 1995, *A&A* **302**, 483.

Stecklum@methusalix.tls-tautenburg.de
(Bringfried Stecklum)
hukaufl@eso.org

The Reflex Cluster Survey: Observing Strategy and First Results on Large-Scale Structure

L. GUZZO[1], H. BÖHRINGER[2], P. SCHUECKER[2], C.A. COLLINS[3], S. SCHINDLER[3], D.M. NEUMANN[4], S. DE GRANDI[1], R. CRUDDACE[5], G. CHINCARINI[1,6], A.C. EDGE[7], P.A. SHAVER[8], W. VOGES[2]

[1]*Osservatorio Astronomico di Brera, Milano/Merate, Italy*
[2]*Max-Planck-Institut für Extraterrestrische Physik, Garching, Germany*
[3]*Liverpool John Moores University, Liverpool, U.K.*
[4]*CEA Saclay, Service d'Astrophysique, Gif-sur-Yvette, France*
[5]*Naval Research Laboratory, Washington D.C., U.S.A.*
[6]*Dipartimento di Fisica, Università degli Studi di Milano, Italy*
[7]*Physics Department, University of Durham, U.K.*
[8]*European Southern Observatory, Garching, Germany*

1. Introduction

As a modern version of ancient cartographers, during the last 20 years cosmologists have been able to construct more and more detailed maps of the large-scale structure of the Universe, as delineated by the distribution of galaxies in space. This has been possible through the development of redshift surveys, whose efficiency in covering ever larger volumes has increased exponentially thanks to the parallel evolution in the performances of spectrographs and detectors (see e.g. Da Costa 1998 and Chincarini & Guzzo 1998, for recent reviews of the historical development of this field).

While the most recent projects, as the Las Campanas Redshift Survey (LCRS, Shectman et al. 1996) and the ESO Slice Project (ESP, Vettolani et al. 1997) have considerably enlarged our view by collecting several thousands of redshifts out to a depth of $\sim 500\ h^{-1}$ Mpc[1], the quest for mapping a "fair sample" of the Universe is not yet fully over. These modern galaxy redshift surveys have indeed been able to show for the first time that large-scale structures such as superclusters and voids keep sizes that are smaller than those of the surveys themselves (i.e. $\sim$ 100–200 h^{-1} Mpc). This is

[1]Here h is the Hubble constant in units of 100 km s^{-1} Mpc^{-1}.

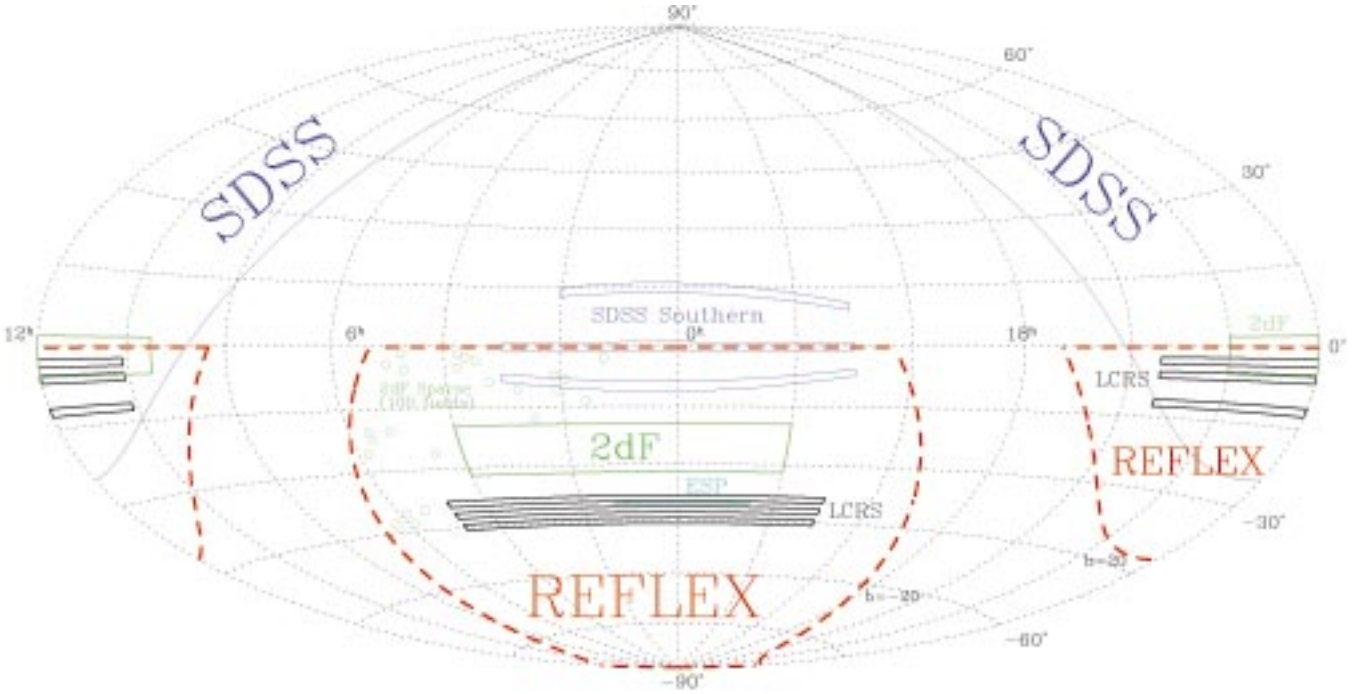

Figure 1: Aitoff view of how wide-angle redshift surveys with typical depth of $z \sim 0.2$ are covering the available sky (see Guzzo 1999 for details).

in contrast to the situation only a few years ago, when every new redshift survey used to discover newer and larger structures (a famous case was the "Great Wall", spanning the whole angular extension of the CfA2 survey, see Geller & Huchra 1989). On the other hand, it has also been realised from the ESP and LCRS results, among others, that to characterise statistically the scales where the Universe is still showing some level of inhomogeneity, surveys covering much larger areas to a similar depth ($z \sim 0.2$), are necessary.

To fulfil this need, on one side two very ambitious galaxy survey projects have started[2], the Sloan Digital Sky Survey (SDSS, Margon 1998) and the 2dF Redshift Survey (Colless 1999). The SDSS in particular, including both a photometric survey in five filters and a redshift survey of a million galaxies over the whole North Galactic cap, represents a massive effort involving the construction of a dedicated telescope with specialised camera and spectrograph.

Alternatively, one could try to cover similar volumes using a different tracer of large-scale structure, one requiring a more modest investment in telescope time, so that a survey can be performed using standard instrumentation and within the restrictions of public telescopes as those of ESO. This has been the strategy of the REFLEX Key Programme, which uses clusters of galaxies to cover, in the Southern Hemisphere, a volume of the Universe comparable to that of the SDSS in the North. Clusters, being rarer than galaxies, are evidently more efficient tracers for mapping very large volumes. The price to pay is obviously that of loosing resolution in the description of the small-scale details of large-scale structure. However, such information is already provided by the present generation of galaxy surveys.

The REFLEX cluster survey, in particular, is based on clusters selected through their X-ray emission, which is a more direct probe of their mass content than simple counts of galaxies, i.e. richness. Therefore, by using clusters as tracers of large-scale structure, not only do we sample very large scales in an observationally efficient way, but if we select them through their X-ray emission, we also have a more direct relation between luminosity and mass. Further benefits of the extra information provided by the X-ray emission have been discussed in our previous *Messenger* article (Böhringer et al. 1998). In the same paper, we also presented details on the cluster selection, the procedure for measuring X-ray fluxes, and some properties of the objects in the catalogue, as the X-ray luminosity function, together with a first determination of the power spectrum. Results on the cluster X-ray luminosity function have also been obtained during the development of the project from an early pilot subsample at bright fluxes (see De Grandi et al. 1999). Here we would like to concentrate on the key features of the optical follow-up observations at ESO, and then present more results on the large-scale distribution of REFLEX clusters and their clustering properties. Nevertheless, for the sake of clarity we shall first briefly summarise the general features of the survey.

2. The REFLEX Cluster Survey

The REFLEX (ROSAT-ESO Flux Limited X-ray) cluster survey combines the X-ray data from the ROSAT All Sky Survey (RASS), and ESO optical observations to construct a complete flux-limited sample of about 700 clusters with measured redshifts and X-ray luminosities. The survey covers almost the southern celestial hemisphere (precisely $\delta < 2.5°$), at galactic latitude $|b_{II}| > 20°$ to avoid high NH column densities and crowding by stars. Figure 1 (reproduced from Guzzo 1999), shows the region covered by the REFLEX survey, together with those of wide-angle galaxy redshift surveys of similar depth, either recently completed (ESP, LCRS), or just started (SDSS, 2dF).

Presently, we have selected a complete sample of 460 clusters to a nominal flux limit of 3×10^{-12} erg s^{-1} cm^{-2}. Due to the varying RASS exposure time and interstellar absorption over the sky, when a simultaneous requirement of a minimum number of source counts is applied, some parts of the sky may reach a lower flux. For example, when computing the preliminary REFLEX luminosity function presented in Böhringer et al. (1998), a threshold of 30 source counts in the ROSAT hard band was set, which resulted in a slightly reduced flux limit over 21.5% of the survey area. The important point to be made is that a full map of these variations is known as a function of angular position and is exactly accounted for in all the statistical analyses.

This first sample, upon which the discussion on clustering and large-scale structure presented here is based, has been constructed to be at least 90% complete, as described in Böhringer et al. (1998). Several external checks, as comparisons with independently extracted sets of clusters, support this figure. The careful reader may have noticed that the total number of objects in this sample has

[2]An earlier pioneering attempt in this direction was the Muenster Redshift Project, which used objective-prism spectra to collect low-resolution redshifts for a few hundred thousand galaxies (see e.g. Schuecker et al. 1996).

been reduced by 15 since the time of writing our previous *Messenger* report. This is the result of the ongoing process of final identification and redshift measurement: spectroscopy and detailed deblending of X-ray sources have led to a reclassification of 15 X-ray sources which either had AGN counterparts or fell below the flux limit. With these new numbers, as of today 95% of the 460 candidates in this sample are confirmed and observed spectroscopically. Final clearing up and measurement of redshifts for the remaining $\sim$ 20 candidates is foreseen for a forthcoming observing run next May. In the following, we shall simply refer to this complete sample as the "REFLEX sample". The distribution on the sky of the REFLEX clusters defined in this way is shown in Figure 2.

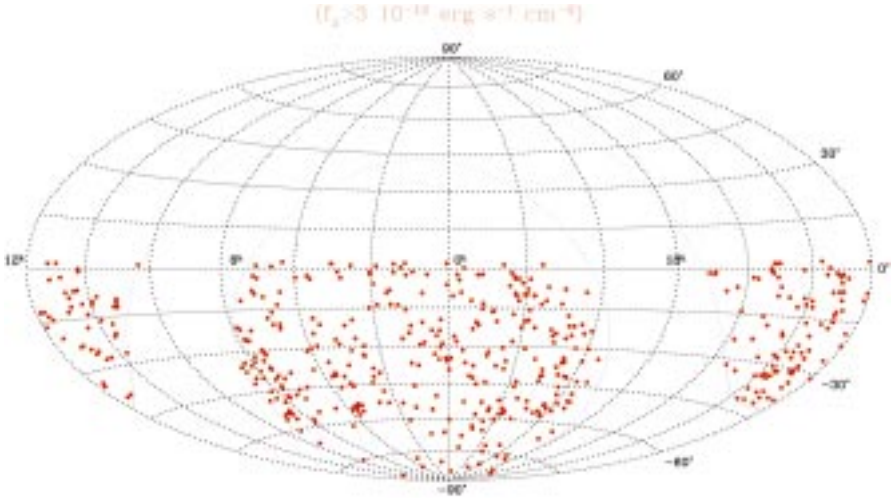

Figure 2: The distribution on the sky of the clusters in the REFLEX sample with $f_X \geq 3 \times 10^{-12}$ erg s^{-1} cm^{-2}. Note that the area around the Magellanic Clouds ($\alpha \sim 1^h$ and $\sim 5^h$, $\delta \sim -70°$), is not included in the survey.

3. Optical Follow-up Observing Strategy

The follow-up optical observations of REFLEX clusters were started at ESO in 1992, under the status of a Key Programme. The goal of these observations was twofold: (a) obtain a definitive identification of ambiguous candidates; (b) obtain a measurement of the mean cluster redshift.

First, a number of candidate clusters required direct CCD imaging and/or spectroscopy to be safely included in the sample. For example, candidates characterised by a poor appearance on the Sky Survey IIIa-J plates, with no dominant central galaxy or featuring a point-like X-ray emission had to pass further investigation. In this case, either the object at the X-ray peak was studied spectroscopically, or a short CCD image plus a spectrum of the 2–3 objects nearest to the peak of the X-ray emission was taken. This operation was preferentially scheduled for the two smaller telescopes (1.5 m and 2.2 m, see below), and was necessary to be fully sure of keeping the completeness of the selected sample close to the desired value of 90%. In this way, a number of AGN's were discovered and rejected from the main list.

Once a cluster was identified, the main scope of the optical observations was then to secure a reliable redshift. The observing strategy was designed so as to compromise between the desire of having several redshifts per cluster, coping with the multiplexing limits of the available instrumentation, and the large number of clusters to be measured. Previous experience on a similar survey of EDCC clusters (Collins et al. 1995) had shown the importance of not relying on just one or two galaxies to measure the cluster redshift, especially for clusters without a dominant cD galaxy. EFOSC1 in MOS mode was a perfect instrument for getting quick redshift measurements for 10–15 galaxies at once, but only for systems that could reasonably fit within the small field of view of the instrument (5.2 arcmin in imaging with the Tektronics CCD #26, but less than 3 arcmin for spectroscopy in MOS mode, due to hardware/software limitations in the use of the MOS masks). This feature clearly made this combination useful only for clusters above $z = 0.1$, i.e. where at least the core region could be accommodated within the available area.

The other important aspect of using such an instrumental set-up is that in several cases, after removal of background/foreground objects, one is still left with 8–10 galaxy redshifts within the cluster, by which a first estimate of the cluster velocity dispersion can be attempted. This clearly represents further, extremely important information related to the cluster mass, especially when coupled to the X-ray luminosity available for all these objects.

At smaller redshifts, doing efficient multi-object spectroscopy work would have required a MOS spectrograph with a larger field of view, i.e. 20–30 arcminutes diameter. One possible choice could have been the fibre spectrograph Optopus (Avila et al. 1989), but its efficiency in terms of numbers of targets observable per night was too low for covering several hundred clusters as we had in our sample. The best solution in terms of telescope allocation pressure and performances was found in using single-slit spectroscopy and splitting the work between the 1.5-m and 2.2-m telescopes. Clearly, this re-

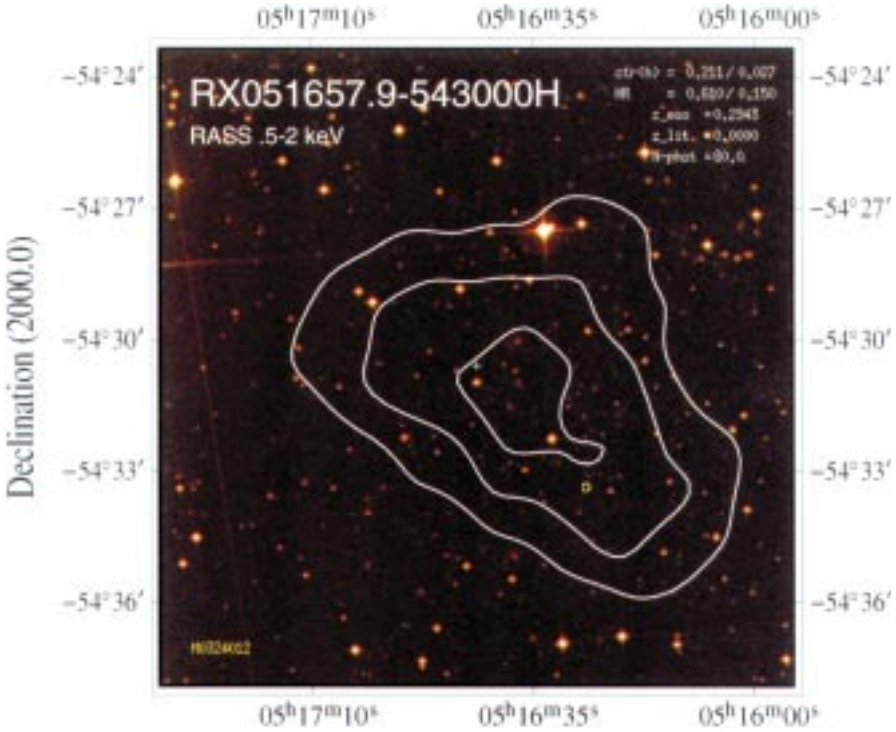

Figure 3: 15 × 15 arcmin identification image of a REFLEX cluster at z = 0.294. The optical image is from the Digitised Sky Survey (DSS), with superimposed the X-ray contours from the RASS. As suggested by the contours, this X-ray source shows a statistically significant extension.

Figure 4: Short CCD exposure (~ 60 sec, no filter) taken with EFOSC1 at the 3.6-m telescope, covering the central region of the REFLEX cluster of previous figure. The field side is 5.2 arcmin. Note the remarkable glory of faint galaxies around the central brightest members. The numbers indicate the positions of the slitlets for the MOS observations.

quired accepting some compromise in our wishes of having multiple redshifts, so that at the time of writing about 30% of the clusters observed at ESO have a measure based on less than 3 redshifts. The reliability of these as estimators of the cluster systemic velocity, however, is significantly enhanced by the coupling of the galaxy positions with the X-ray contours: we can clearly evaluate which galaxies have the highest probability to be cluster members. This is another advantage of a survey of X-ray clusters over optically selected clusters. At the time of writing, in about seven years of work, we have observed spectroscopically a total of about 500 cluster candidates, collecting over 3200 galaxy spectra.

Figure 3 shows one example of the identification images, used for the first confirmation of the candidates. These pictures are constructed for all our candidates by combining the Digitised Sky Survey plates of the ESO/SRC atlas (image) and the RASS X-ray data (contours). Although this cluster (RX051657.9-543000), lies at a redshift $z = 0.294$ (close to the redshift identification limit of REFLEX at $z = 0.32$), a sufficient number of galaxies is detected in the optical image even at the depth of the survey plates. This picture gives a clear example of how the X-ray contours "guide the eye" in showing which are the "best" galaxies to be observed. In this case we had a MOS observation, but had we observed only the central two galaxies within the X-ray peak, we would have obtained a correct estimate of the cluster redshift.

The same cluster is then visible in the direct EFOSC1 image of Figure 4. This is a short service exposure (less than one minute), taken in white light as a template for the drilling of the slits on the EFOSC1 MOS mask. The image shows a spectacular abundance of faint galaxies, one of the most impressive cases observed during our survey.

After looking at this latest picture, it is natural to ask what is, for example, the galaxy luminosity function of this cluster, or what are the colours of this large population of faint objects. This is clearly important information, which at the moment, however, is only available for a restricted fraction of REFLEX clusters (Molinari et al. 1998). To cover this aspect, a wide-field imaging campaign is going to commence in the next semester, starting first with those medium-redshift clusters that best match the WFI at the 2.2-m telescope.

4. The Large-Scale Distribution of X-Ray Clusters

The cone diagram of Figure 5 plots the distribution of REFLEX clusters in the South Galactic cap area of the survey, selecting only objects with $z < 0.2$ and $\delta > -55°$, to ease visualisation. One can easily notice a number of superstructures with sizes $\sim 100\ h^{-1}$ Mpc, that show explicitly the typical scales on which the cluster distribution is still inhomogeneous.

This inhomogeneity can be quantified at the simplest level through the two-point correlation function $\xi(s)$, that measures the probability in excess of random of finding a pair of clusters with a given separation (the variable s is used here to indicate separations in redshift space). A preliminary estimate of $\xi(s)$ for the REFLEX sample is shown by the filled circles in Figure 6. The dashed line shows for comparison the Fourier transform of a simple fit to the power spectrum P(k) measured from a subsample of the same data (see Böhringer et al. 1998). The estimates of $\xi(s)$ and P(k) were performed

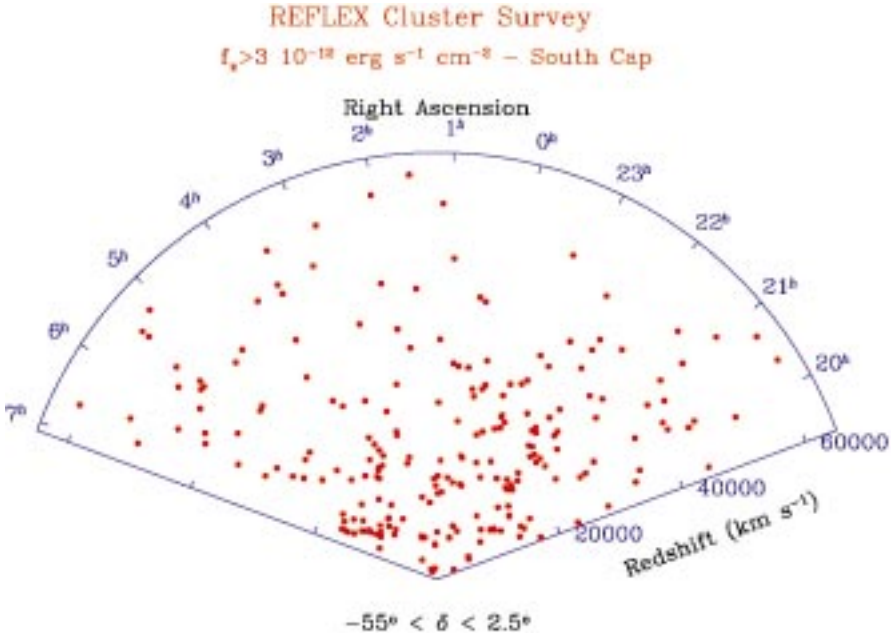

Figure 5: The large-scale distribution of REFLEX clusters within part of the South Galactic cap region. Only objects North of $\delta = -55$ are shown, to avoid excessive confusion by the projection along declination.

by taking into account the angular dependence of the survey sensitivity, i.e., the exposure map of the ROSAT All-Sky Survey, and the NH map of galactic absorption. The good agreement between the two curves is on one hand an indication of the self-consistency of the two estimators applied in redshift and Fourier space. Also, it shows a remarkable stability in the clustering properties of the sample, given that for the measure of P(k) the data were conservatively truncated at a comoving distance of 200 h^{-1} Mpc (Schuecker et al., in preparation), while the estimate of ξ(s) uses the whole catalogue (Collins et al., in preparation). On the other hand, this also indicates that the bulk of the clustering signal on ξ(s) is produced within the inner 200 h^{-1} Mpc of the survey, which is expected because this is the most densely sampled part of the flux-limited sample. We shall explore this in more detail when studying volume-limited samples, with well-defined lower threshold in X-ray luminosity.

Figure 6 shows that ξ(s) for clusters of galaxies is fairly well described by a power law out to 40 h^{-1} Mpc, and then breaks down, crossing the zero value around 50 h^{-1} Mpc. It is interesting to compare it with the two-point correlation function of galaxies, as we do in Figure 7. The galaxy data shown here (points) are obtained from two volume-limited subsamples of the ESP survey (Guzzo et al. 1999). They are compared to ξ(s) from the REFLEX clusters, given by the dashed lines. To ease the comparison, we preferred to plot the curves of ξ(s) as computed from the Fourier transform of P(k). This is given by the top line, while the bottom line has been re-scaled by a factor $b_c^2 = (3.3)^2$ in amplitude. This difference in amplitude, or bias, is expected, as clusters represent the high, rare peaks of the galaxy density distribution, and it can be demonstrated (Kaiser 1984) that their clustering has to be enhanced with respect to that of the general field. This quoted value of b_c, however, does not have a direct physical interpretation, as it is obtained from a flux-limited sample, and thus related to clusters having different mean intrinsic luminosities at different distances. One important aspect of selecting clusters through their X-ray emission is in fact that a selection in X-ray luminosity is closer to a selection in rnass, than if one used a measure like the cluster richness (i.e. the number of galaxies within a given radius and a given magnitude range, as in the case of the Abell catalogue). For this reason, the observation that ξ(s) has a different amplitude for volume-limited subsamples with different X-ray luminosity limits (i.e. a different value of b_e), has important implications for the theory (Mo & White 1996). The validity of a simple biasing amplification mechanism on these scales is explicitly supported by the very similar slopes of ξ(s) shown in Figure 7 by galaxies and clusters. A full discussion concerning the luminosity dependence of the amplitude of the correlation function is being prepared (Collins et al., in preparation).

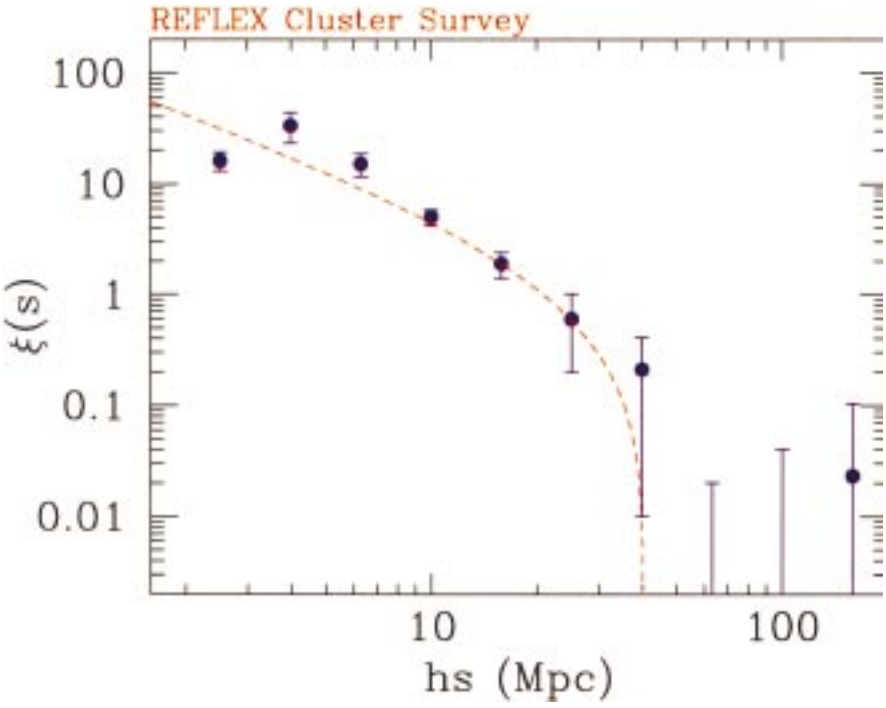

Figure 6: The two-point correlation function of clusters of galaxies in the REFLEX survey. The filled circles give the direct estimate, while the dashed line is computed by Fourier transforming the power spectrum of the survey data, that we showed in Böhringer et al. 1998.

5. Conclusions

We have discussed how after several years of work with the X-ray data from the RASS and with ESO telescopes, the REFLEX project has reached a stage where the first significant results on large-scale structure can be harvested. We hope to have at least given a hint of how the REFLEX survey is possibly the first X-ray selected cluster survey where the highest priority was given to the statistically homogeneous sampling over very large solid angles. This makes it an optimal sample for detecting and quantifying the spatial distribution of the most massive structures in the Universe, as can be appreciated from the high S/N superclusters visible in the cone diagram of Figure 5 out to at least $z \sim 0.1$.

We have also shown how these results have been reached without specially designed instrumentation. Started in May 1992, with the next May run it will be seven years that we have been observing and measuring redshifts for REFLEX clusters. Again, this long timescale is a consequence of the fact that the project is based on "public" instrumentation, and therefore subject to the share of telescope time with the general ESO community. Clearly, even in these terms, this could have never been possible at ESO without the long-term "Key Programme" scheme. In fact, it is exactly for surveys like REFLEX, i.e. large cosmology projects, that the concept of Key Programmes was originally conceived, under suggestion of those few people that at the end of the eighties

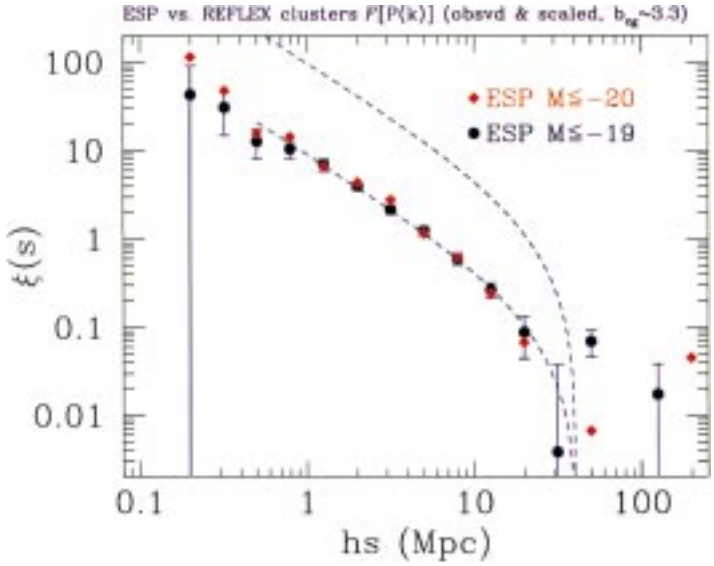

Figure 7: Comparison of the two-point correlation function of REFLEX clusters (top dashed line), to that of ESP galaxies (dots, Guzzo et al. 1999). The bottom dashed line is the REFLEX x(s) after scaling by an arbitrary bias factor of $b_c^2 = (3.3)^2$. The agreement in shape between galaxies and clusters is remarkable.

were starting doing large-scale structure work in continental Europe. If the aim of the Key Programmes was that of making the exploration of the large-scale structure of the Universe feasible for European astronomers, providing them with a way to compete with the dedicated instrumentation of other institutions, we can certainly say that, after ten years, this major goal has probably been reached.

References

Avila, G., D'Odorico, S., Tarenghi, M., & Guzzo, L., 1989, *The Messenger*, **55**, 62.
Böhringer, H. et al., 1998, *The Messenger*, **94**, 21 (astro-ph/9809382).
Chincarini, G., & Guzzo, L., 1998, in *Proc. of V^{eme} Colloque de Cosmologie*, H. De Vega ed., in press.
Colless, M., 1998, Phil. Trans. R. Soc. Lond. A, in press (astro-ph/9804079
Collins. C. A., Guzzo, L., Nichol, R. C., and Lumsden, S. L., 1995, *MNRAS*, **274**, 1071.
Da Costa, L.N., 1998, in *Evolution of Large-Scale Structure: from Recombination to Garching*, T. Banday & R. Sheth eds., in press (astro-ph/9812258).
De Grandi, S., et al., 1999, *ApJ* (Letters), in press (astro-ph/9812423).
Geller, M.J. & Huchra, J.P., 1989, *Science*, **246**, 897.
Guzzo, L., 1999, in *Proc. of XIX Texas Symposium*, (Paris – October 1998), Elsevier, in press.
Guzzo, L., et al. (The ESP Team), 1999, *A&A*, in press (astro-ph/9901378).
Kaiser, N., 1984, *ApJ*, **284**, L9.
Margon, B., 1998, Phil. Trans. R. Soc. Lond. A, in press (astro-ph/9805314).
Mo, H.J., & White, S.D.M., 1996, *MNRAS*, **282**, 347.
Molinari, E., Moretti, A., Chincarini, G., & De Grandi, S., 1998, *A&A*, **338**, 874.
Schuecker, P., Ott, H.-A., & Seitter, W.C., 1996, *ApJ*, **472**, 485.
Shectman, S.A., et al., 1996, *ApJ* **470**, 172.
Vettolani, G., et al. (the ESP Team), 1998, *A&AS*, **130**, 323.

G. Guzzo
guzzo@merate.mi.astro.it

NTT Service Mode Observations of the Lyman-Limit Absorber towards Q1205-30

J.U. FYNBO, B. THOMSEN, P. MØLLER, ESO

1. Introduction

The amount of information about the galaxy population at high redshift (z = 2–4) has increased tremendously in the last few years. Using the Lyman-break technique, several hundred high-redshift star-forming galaxies, Lyman-break galaxies (LBGs), have been detected and studied with imaging and spectroscopy (Steidel et al.,1996). Using the Hubble Space Telescope, detailed morphological studies of the LBGs have been carried out (Dickinson, 1998). It is, however, not yet known how complete the Lyman-break technique is in detecting high-redshift galaxies.

An independent route along which to study the galaxy population at high redshift is via the high column density QSO absorption-line systems. The advantage of high column density QSO absorption-line systems is that a wealth of information on the chemical evolution can be and has been obtained by studying the metallicity and dust content of the absorbers from high-resolution spectroscopic studies of the background QSOs (e.g. Lu et al., 1996). However, the spectroscopic studies will not tell us anything about the emission properties of the absorbing galaxies.

Only when combining the information obtained from the LBG studies (e.g. the luminosity function of LBGs), the absorption-line statistics for QSO absorp-tion-line systems and the properties of galaxy counterparts of QSO absorption-line systems can we hope to disentangle the observational selection biases which each of the different studies suffer from, and obtain a more complete insight into the nature of the high-redshift galaxy population.

We are currently undertaking programmes aimed at identifying galaxy counterparts of the two most gas-rich subgroups of QSO absorption-line systems, Damped Lyα Absorbers (DLAs) and Lyman-limit systems (LLSs). Three out of the five high-redshift DLAs that have been detected in emission at present are at approximately the same redshift as the background QSO. In order to examine whether $z_{abs} \approx z_{em}$ systems indeed are more active emitters (e.g. due to photoionisation by the QSO or induced star formation) we choose to study Q1205-30, since the spectrum of Q1205-30 published by Lanzetta et al. (1991) shows the presence of a strong LLS at the emission redshift of the QSO, which is z_{em} = 3.036.

In this paper we report on preliminary results of our analysis of the data obtained during NTT service observation in January, February and March 1998.

2. Locating Q1205-30

The coordinates of Q1205-30 have not been published (in the paper by Lanzetta et al. (1991) the reference to Q1205-30 is 'Hazard and McMahon, unpublished'). As the coordinates could not be obtained through private communication, we had to 'rediscover' Q1205-30. We found that one way in which this could be accomplished was by obtaining a copy of the prism plate of the area around RA 12^h05^m, DEC –30° from the UK-prism survey. After careful visual inspection of the plate UJ9085P we found a point source with an emission line consistent with being Lyα at $z \approx 3.0$ and measured its approximate coordinates from the plate. By examining the corresponding field in the Digital Sky Survey we measured the precise position of Q1205-30 to be RA 12 05 35.72, DEC –30 14 25.8 (1950).

3. Observations and Data Reduction

We have applied a narrow/broad-band filter technique in several earlier studies of galaxy counter parts of DLAs (e.g. Møller & Warren, 1993, Fynbo, Møller & Warren, 1999). This method is extremely well suited towards service observations since it requires many long integrations of the same field on the sky during dark time. We hence submitted a proposal for and obtained NTT service mode time to image the field of Q1205-30 using a special 20 Å (FWHM) narrow filter centred at 4906 Å which is the wavelength of redshifted Lyα, and in standard B and I filters. The data were obtained during January, February and March, 1998. The total integration times in each filter and the seeing in each of the combined frames are given in Table 1.

Also observed were two standard star fields from Landolt (1992) and the three spectrophotometric standard stars Eggr99, Feige 56 and L970.

The individual reduced images in each of the three filters were combined using the code described in Møller and Warren (1993), which optimises the signal-to-noise for faint objects. We reach 5σ limiting magnitudes of 26.0 in B(AB), 25.1 in I(AB) and 25.1 in the narrow band. At z = 3.036 a narrow-band AB magnitude of 25.1 corresponds to a Lyα flux of 1.0×10^{-17} ergs^{-1} cm^{-2}.

4. Results

4.1 The neighbourhood of Q1205-30

Figure 1 shows the result of the subtraction of the point-spread function (PSF)

Table 1: Journal of observations, NTT, 1998

Filter	Combined seeing (arcsec)	Exposure Time (sec)
CS 4906/20	1.4	64000
B	1.3	3600
I	0.96	5600